Engineering Solid Mechanics 7 (2019) 121-130

Contents lists available at GrowingScience

Engineering Solid Mechanics

homepage: www.GrowingScience.com/esm

Experimental investigation and numerical prediction for the fatigue life durability of austenitic stainless steel at room temperature

M. A. Khairul[a], S. M. Sapuan[a], Faris M. AL-Oqla[b*] and E. S. Zainudin[c]

[a]*Mechanical Engineering Section, Universiti Kuala Lumpur, Malaysia France Institute, Section 14, Jalan Teras Jernang, 43650 Bandar Baru Bangi, Selangor, Malaysia*
[b]*Department of Mechanical Engineering, The Hashemite University, Zarqa 13133, Jordan*
[c]*Institute of Tropical Forestry and Forest Products (INTROP), Putra Universiti, 43400 UPM Serdang Selangor, Malaysia*

ARTICLE INFO

Article history:
Received 26 December, 2018
Accepted 26 February 2019
Available online
11 April 2019

Keywords:
Fatigue life
Composites
Stainless steel
Modelling
Prediction

ABSTRACT

This work investigated and predicted the fatigue life durability of Austenitic Stainless Steel 316L at room temperature due to its importance in plant industries worldwide. Modelling and simulations were performed to clarify the fracture as well as stress distribution using integrated mechanism. Experimental fatigue validations were also carried out to demonstrate the effect of various fatigue life parameters. Various loading conditions with variable load amplitudes were validated utilizing a frequency of 5 Hz and a stress ratio of 0.1. The accuracy of the simulation results were also verified based on the experimental data. High consistencies between the predicted fatigue life and the experimental results were achieved which increases the validity of the built model.

1. Introduction

Due to the tremendous need for engineers to properly select and use the most appropriate function as well as economic material type to achive successful design, further investigations on the materials behaviour and fracture under different conditions are still desired (Yıldız et al. 2011, Mughrabi 2001, Huynh et al. 2008, Khairul et al. 2017). The new available types of modern materials including both traditional and green ones (Al-Oqla et al. 2014; 2015a,b; Al-Oqla and Sapuan 2015) which make the selection of the appropriate material type a sophisticated problem (Al-Oqla and Sapuan 2018; Al-Oqla 2017; Al-Oqla and Salit 2017 Al-Oqla et al. 2015c). A few decades ago, the prevailing viewpoint was brittle material did not experience fatigue (as brittle materials have limited dislocation motion); however, brittle materials exhibit both mechanical fatigue and thermal fatigue under repetitive loadings. In addition, there are still various failures of components in many heavy industries in global market, including the fabrication stage of components. This phenomenon is mainly due to the development of natural defect that is not completely avoidable, such as inhomogeneity and non-metallic inclusions (Al-Oqla et al., 2019; Fares et al., 2019). In heavy industries such as power plant, aerospace field, and oil and gas industries, the component that is made of material such as 316L stainless steel is frequently used in

* Corresponding author.
E-mail addresses: fmaloqla@hu.edu.jo (F. M. AL-Oqla)

doi: 10.5267/j.esm.2019.4.001

both room and high temperature conditions. Many stainless steel grades have been employed to satisfy the performance requirements in many fields, such as aerospace, automotive, medical, electronic, and energy industries, as well as oil and gas industries. Different types of austenitic stainless steel is currently being employed in various industries, such as the oil and gas industries and nuclear industries, i.e., type 304, 309, 316L, 321, 347, 348, and 316LN, whereas stainless steel 316L is more convenient considering its advantages. The elevated temperature and stress-creep the deformation of component engineering that has given significant impact to the world (Mughrabi 2001; Hayhurst 1972; Finnie and Heller 1959; Bendersky et al. 1985). Several researchers have studied and investigated the factors that contributed to the cumulative damage mechanisms as they are significant in considering the effect of diversity in types of creep damage on high stress fatigue behaviour, shape, and high temperature. Stainless steel experienced severe thermal cycles in high heat flux application in transportation oil systems. Many researchers have focused on the service life prediction and extension of tubular steel, which was challenging due to the geometric shapes of specimens and the complexity of the phenomena. Concerning to determination and characterization of accuracy of a life prediction, both the upper bound and the lower bound were introduced as main aspects of engineering components at elevated temperatures. However, no specific life prediction model had gained global acceptance among the majority of plant industries. It was discovered that each industry performed separate life predictions according to the situation and application. The notable difficulty in the prediction on any material was accounting for the contributions by creep and/or environmental attack of the fatigue process (Mughrabi 2001; Hayhurst 1972; Finnie and Heller 1959; Bendersky et al. 1985). Several investigations have been performed to study the effect of creep, temperatures on the mechanical characteristics of steel. Tabuchi and co-workers (2003) have mentioned that the high strength steels are usually operated at room temperature and stresses below the yield strength and failure would occur for such types of steel due to the influences of creep stresses as well as other environmental factors. On the other hand, Zheng et al. (2005) have reported that the petroleum and natural gas transmission that utilize stainless steel as pipelines will contain defects and flaws from the manufacturing installation and servicing process. These defects could influence the safety of pipelines and even reduce their service life which might goes to massive financial costs and endanger the ambient ecological circumstances. In the damage tolerant design approach for any structural component, analysis and testing should be performed to demonstrate whether any pre-existing defects in the material will grow to catastrophic proportions within a time span of half the inspection interval. This testing necessitates an accurate prediction of the fatigue crack growth rate for any given service conditions that pertain to the criticality of the loading and temperature conditions for the component. Therefore, considerable effort towards an understanding of crack growth behaviour under fatigue loading with elevated temperatures and the relevance of these mechanics to the failure of a structure caused by creep, fatigue and the environment's effects, such as oxidation is crucial Fan et al. (2005). Also creep-fatigue, oxidation fatigue and creep-fatigue-oxidation damage to components were studied based on the specific materials and loading conditions Beden et al. (2009). Moreover, several studies o suggested damage models based on endurance limit reduction were proposed to study the fatigue behaviour of steel. The creep-fatigue evaluation methods have been proposed based on fatigue life and failure mechanisms under creep-fatigue loading. Two main life prediction methods, namely, an empirical "linear damage summation" method and a mechanism-based "cavitation damage" model were frequently used (Fan et al. 2006). These models were nonlinear and account for the load sequence effect (Marquis et al. 2013). Coarse slip model on the other hand was also considered to be an avalanche of fine movements, whereas slip lines appear as parallel lines or bands within a grain when viewed perpendicular to a free surface (Niesłony et al. 2012). However, none of these models considered the load interaction effect (Stephens et al. 2000).

Consequently, the estimation of steel life and verifying the effectiveness of particular parameters and factors on the steel structures to improve the development of this modern arena are still required. Moreover, proper investigations and simulating various conditions that affect the life span of such types of materials are of paramount importance. Thus, the objective of this work is to properly investigate the effect of various parameters that affect the life span of Austenitic Stainless Steel 316L due to cyclic

loading and to predict such life using a FEA model as well as to validate the prediction with experimental fatigue tests to demonstrate such effects under various loading conditions.

2. Materials and Design

Experimental specimens from austenitic 316L stainless steel were supplied and fabricated by S.N Machinery Services Sdn. Bhd. in Malaysia to be utilized in the fatigue's experiment. The specimen provided was a 26.7 mm diameter cold drawn bar, annealed at 1100°C and water quenched and was fabricated to be an hourglass shaped specimen which has threaded ends inside for gripping purposes in accordance to the ASTM 606 for fatigue test. The grain size was 80 μm for 316L stainless steel for the heat treatment. To collect the data for the fatigue test, seven data plots were sufficiently adequate, as recommended by ASTM E606-92 (1998) to establish an S-N curve. The specimens were subjected to several different maximum stress levels with an initial stress of 0.9 YS (90% of the yield strength) of the materials followed by 0.80 YS, 0.70 YS, 0.60 YS, 0.50 YS, 0.40 YS and 0.30 YS. The magnitude of load was inserted and the distribution of load was selected to be uniform. The periodic was chosen as the type of amplitude of a sinusoidal. The time span was set as step time, circular frequency, $2\pi f$ with 31.42 as the frequency was set to 5Hz, starting time and initial amplitude as zero. The specimens were subjected to repetitive loads to impose a limit of fatigue life for 10^7 cycles due to the cost and time constraint/limitation.

3. Fatigue Experimental Work

Fatigue is considered one of the most serious failure modes of materials due to the effect of repeated cyclic stresses for a period of time. It is influenced by various factors, for instance, size, shape and design of the component, conditions of the surface or operating environment. Seven specimens were involved in the fatigue test with stress ratio of 0.1 and 5 Hz of loading frequency in the investigation of the effect of such factors on the Austenitic Stainless Steel 316L at room temperature. Fatigue tests were conducted using Hydraulic Universal testing Machine (model: Instron 8802) with 250 kN load capacity. The fatigue machine and set-up experiment with software were shown in Fig. 1. The hourglass specimens of stainless steel with gauge length of 100 mm were used, and results were measured using an extensometer attached at the machine. Test on the Specimens were conducted until rupture stage. The final results were taken as load versus cycles on specimens. Tests were carried out under stress controlled displacement conditions, where sinusoidal waveform is subjected to seven specimens to increase the reliability of the study.

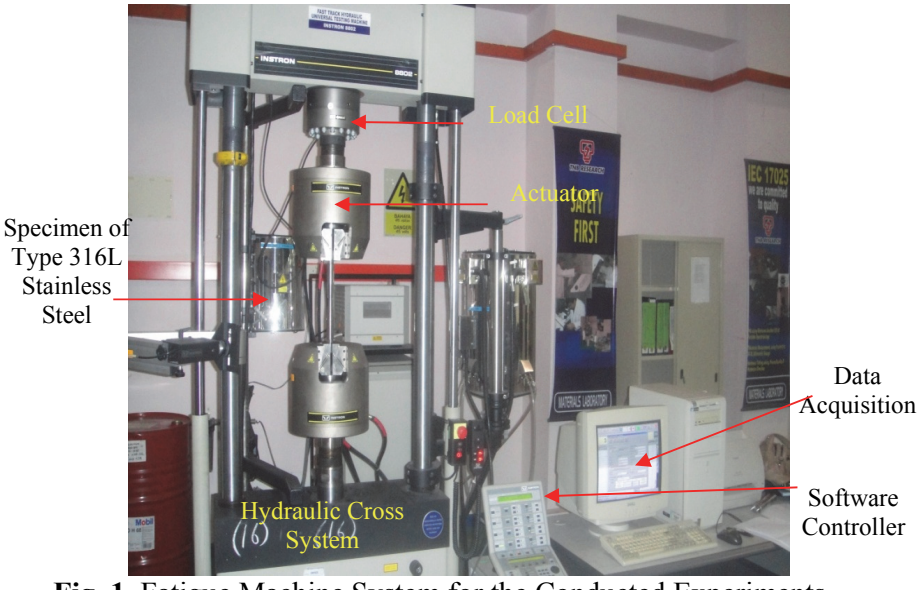

Fig. 1. Fatigue Machine System for the Conducted Experiments.

4. Simulations

A model has been developed using CATIA V5 software. Then, it was imported to ABAQUS software to perform the simulation analysis. This study was carried out to predict the durability of stainless steel 316L steel using Finite Element Analysis (FEA). Fatigue life correlations were incorporated into FEA parameters (Yıldız et al. 2011). The simulated results were validated with experimental data, where the differences between the predicted fatigue life and the experimental fatigue life were discussed. The model was meshed before job analysis was carried out. Upon completion, the post processing results of loads versus cycles were compared with the experimental results as they exhibit well interpretation of the load-cycles responses with experimental at the end of simulations. Specimens were set by elastic materials that are of homogeneous type. The mechanical properties such as density, yield strength, ultimate strength, and Poisson's ratio were inserted into the FEA for initial step as basic properties of specimens. Boundary conditions were used to constrain the model. Boundary conditions for the axisymmetric model were applied, where symmetry on the nodes located at the centre of the gauge length was applied with prescribed displacements on the top part of the model and a predefined temperature as 27^{o}C field along the gauge section on each element. Such constraints were able to create simply supported or fixed conditions. The model utilized axisymmetric eight-node elements. Symmetry of the model was assumed and only the upper half of the specimens was needed to be modelled. The magnitude of the load was inserted and the distribution of load was selected to be uniform. The values were determined according to the percentage of ultimate strength such as 90%, 80%, 70%, 60%, 50%, 40%, and 30% of ultimate strength. The periodic was chosen as the type of amplitude of a sinusoidal. The time span was set as step time, circular frequency, $2\pi f$ with 31.42 as the frequency was set to 5Hz, starting time and initial amplitude as 0. A tubular cylindrically shaped specimen was designed for the fatigue test with a minimum waist of 19.58 mm, a gage length of 40 mm, an outside diameter of 26.7 mm, and a wall thickness of 2 mm. The technique to mesh a model or model region, in which pre-established mesh patterns was applied to particular model topologies. This FE model represents the gauge section of the rounded specimens, and the mesh density provided suitable aspect ratios and accurate numeric results.

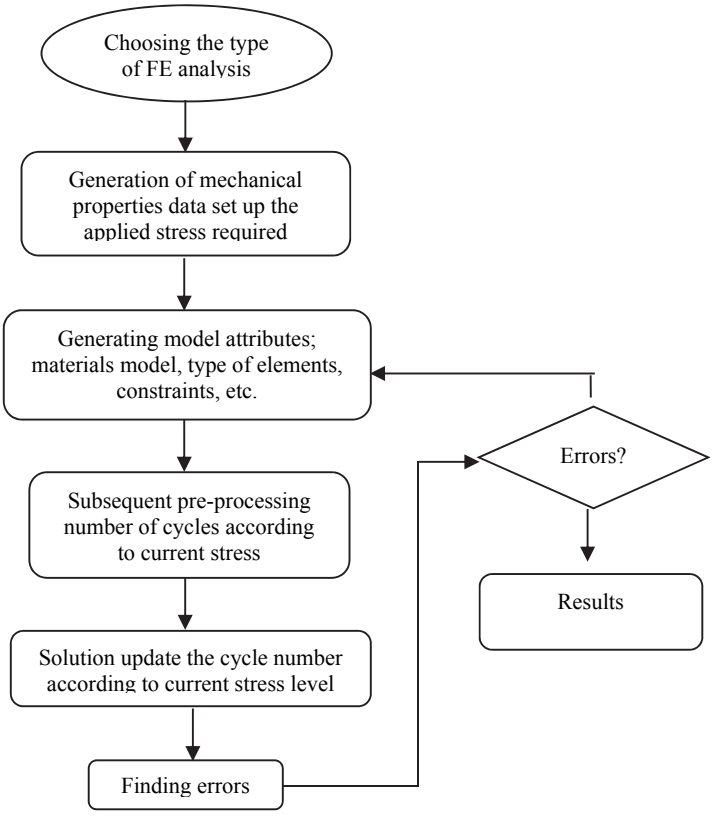

Fig. 2: Flow chart of the conducted simulations

The model considered a tubular specimen that was subjected to an external stress loading and a temperature of 27°C. The test of the model compared the behaviour of the model with the actual problem and its environment. This work focused on the formulation of the model for this system/problem and identified as well as collected the data required to test the model. It also determined the randomness of the input parameter, the number of experiments, the run period and the methodology. Fig. 2 demonstrates the flow chart in running the simulations in order to obtain the cycles to failure of specimen in the current FE analysis.

5. Results and Discussion

The fatigue data of constant amplitude load fatigue analysis with load ratio of 0.1 and frequency of 5 Hz was applied on AISI Type 316L stainless steel specimen. The results of Von Mises stress after the maximum cycles of 8405 was considered when reached to the maximum stress of 315.5 MPa as the highest stress concentration. The failure mechanism map that defines the regions of fatigue failure, creep failure and creep fatigue interaction is shown in Fig. 3.

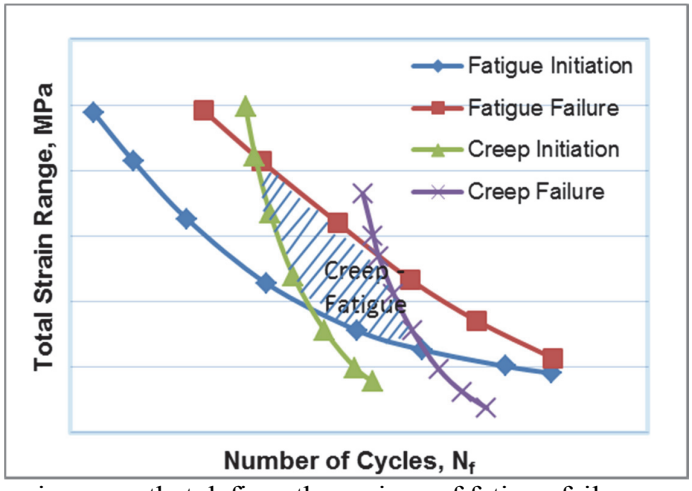

Fig. 3. Failure mechanism map that defines the regions of fatigue failure, creep failure and creep fatigue interaction

Besides that, the region also experienced maximum strain as the maximum stress exerted on the region is stretched out. Thus, the region with the highest stress and strain concentration area will elongate and form crack until it break after exceeding ultimate strength. This statement is supported by Huynh et al. (2008), where most cracks were more susceptible to occur in the high tension zones, normally at a flaw or defect in the base material. This was inconsistence of the expected trend, where the crack is a result of fatigue occurring in the high stress concentration area (Huynh et al., 2008; Maeng & Kang 1999). On the other hand, both ends of specimen with blue colour region undergone the minimum stress and strain, as one end is fixed, whereas the load is applied on the other end. According to the experimental results, the maximum stress was also exerted on the same region. This is because, the thickness of the middle region was the smallest with difference of 3.56 mm compared to other areas and the curve geometry at the region which made it easier for high stress concentration to occur. So, that region is more susceptible to fatigue when cyclic load is applied. Thus, this has proven that the result from the FEA was reliable.

Furthermore, as the 316L stainless steel is a ductile material where it is able to yield under continuous loading at normal temperature, the stress-strain data that was taken from node 1202 in the specimen indicates that it fell under the stress concentration region. A comparison of stress-strain between simulated and experimental cases was as demonstrated in Fig. 4. The yield strength in the simulation and experimental analysis are 463 MPa and 332 MPa, which has a moderate difference, about 131 MPa. According to Velay et al. (2002), there are several aspects that is useful to explain the differences between

calculated and experimental results. These differences are mainly due to the failure of the bulk temperature distribution consideration in simulation, where temperature enhanced creep in specimens, incomplete simulation model formulation, and errors in the experimental strain measurements (Velay et al. 2002). The linear portion of the curve was the elastic region and the slope is the modulus of elasticity or Young's Modulus. The Young's modulus calculated in the simulation was 197 GPa, whereas the experimental Young's modulus was 200 GPa.

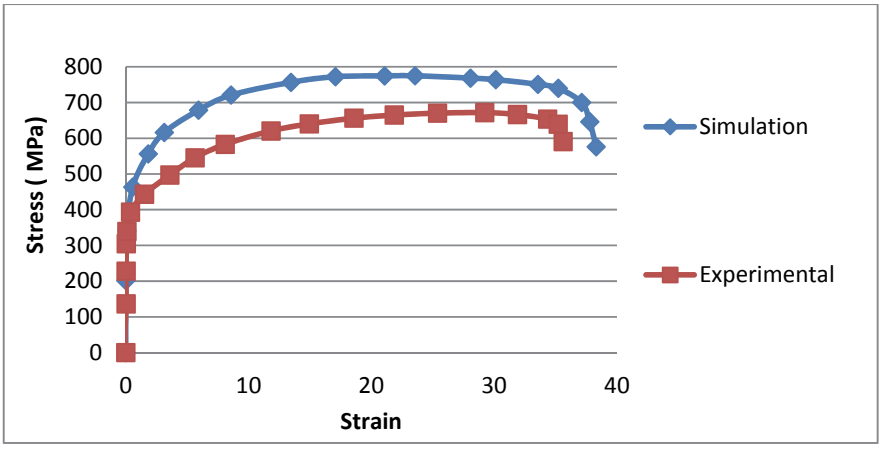

Fig. 4. Average Stress-Strain curve by simulation for Type 316LStainless Steel at room temperature

The S-N curve comparison of simulation data with predicted fatigue lives for Type 316L Stainless Steel is demonstrated in Fig. 5, where there are no failures observed before 8×10^3 cycles and simulation were terminated after 9×10^6 cycles. However, Basquin analysis was used for comparison with the simulation analysis data in order to perform validation study of the model. Generally, the predicted curve of Basquin analysis was slightly lower than the experimental data. The fatigue limit observed in the range of 104 to 107 cycles at maximum stress gave approximately 315 MPa for simulation data, meanwhile 262 MPa for Basquin predicted data. Failures were observed starting from 8×10^3 cycles and the limit of analysis ended at 9×10^6cycles in accordance with the limitation of the number of cycles for the experiment and the validation of the simulation results. According to Beden et al. (2009), the lower fatigue limit predicted compared to simulation can be due to the inherent micro-structural in homogeneity of the material properties, surface difference, the test environment and other factors**.**

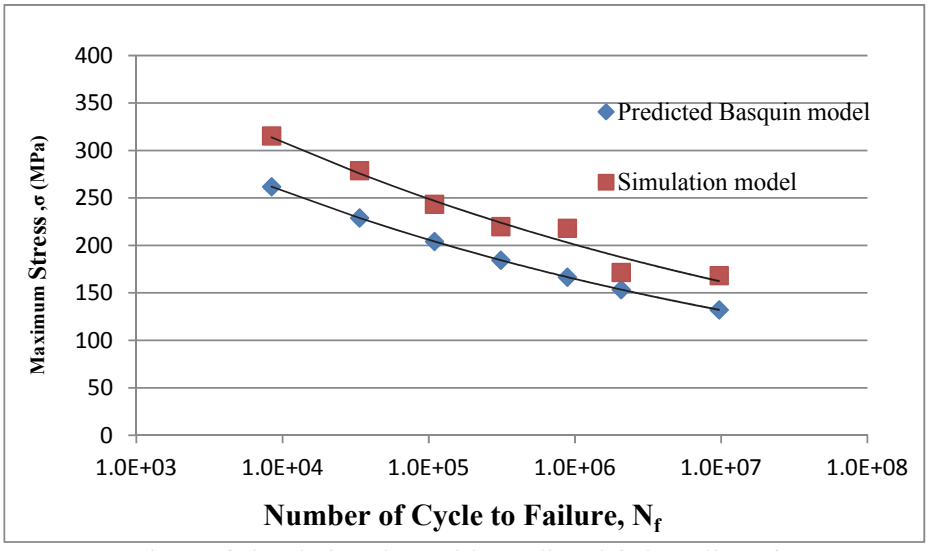

Fig. 5. S-N curve comparison of simulation data with predicted fatigue lives for Type 316L Stainless Steel at room temperature

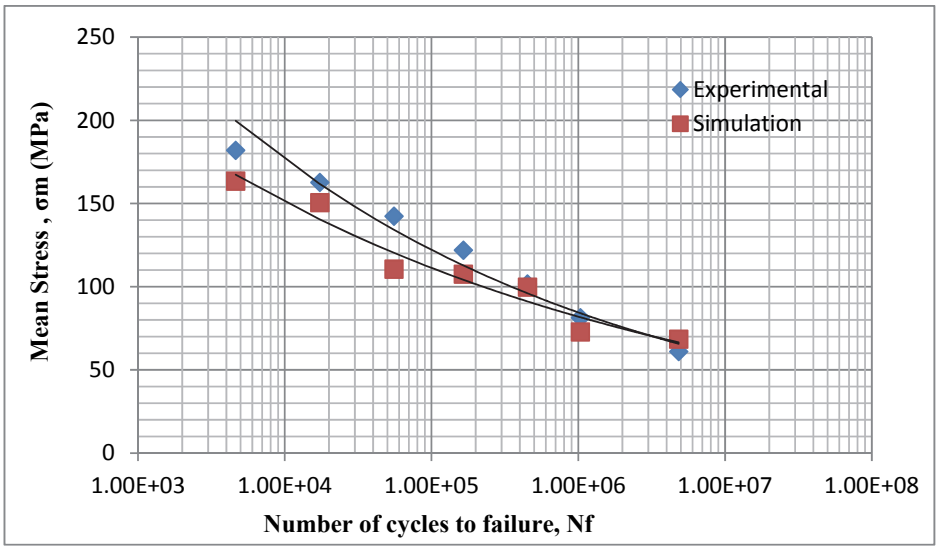

Fig. 6. Mean stress curve comparison of simulation data with predicted fatigue lives for Type 316L Stainless Steel

On the other hand, the mean stress curves comparison of simulation data with the predicted fatigue lives for Type 316L Stainless Steel was interpreted in Fig. 6. The curves represented mean stress for simulation and experimental for comparison of both curves with the line of power law to obtain the discrepancy of stress value results in fatigue life of 182 MPa and 163 MPa, respectively at 4,628 cycles. The comparison of the fatigue performance shown in the two curves under continuous cycling indicated that the simulation data revealed a shorter fatigue life at low stress and a long fatigue life at higher stress than the experimental life of steel. The results for the steel alloys had much higher strength (and lower ductility) than the predicted data, which supposedly result in longer fatigue lives at lower stress ranges for this material. This might imply that the steel exhibit enhanced sensitivity to the development of micro cracks, which control the fatigue behaviour.

In order to validate the simulation results, both experimental and simulation results were further compared with previous FE models for different materials. For instance, the simulation results of stainless steel 316L were compared with the experimental and simulation results of aluminium alloy HS6061-T6 material found by Lu et al. (2011). It is interesting to note that, the maximum stress of the simulation and the experimental data by Lu were 140 MPa and 150 MPa, whereas the maximum stress on simulation of stainless steel 316L was 315 MPa. The significant difference of the maximum stress observed was believed to be due to the different material and the shape of the specimens in terms of machining to cylindrical or plate forms Lu et al. (2011).

The Basquin relation is the general equation which representing typical S-N curve and its expression developed from log–log S-N graphs. According to Niesłony et al. (2012), this equation was usable in the stress-based approach to fatigue analysis and design as it can be used to determine the numbers of cycles to the fatigue crack initiation (Niesłony et al. 2012). The maximum tensile stress for fully reversed loading is given by

$$\sigma_{\max} = \sigma_a = \sigma_f^{'}(2N_f)^b, \tag{1}$$

where $\sigma_f^{'} = 586$ MPa(cycl.)$^{-b}$ for fatigue strength coefficient (for most metals $=\sigma_f$, the true fracture strength), b = -0.142 defined by Raman and Radhakrishnan (2002), which similar value appeared in

previous research for application of stainless steel in plant industries, and N_f is number of cycles to failure (Raman & Radhakrishnan 2002).

Table 1 shows the fatigue life obtained in terms of number of cycles to failure. The load ratio of 0.1 was taken for calculating the mean stress and stress amplitude. It indicated that the overall maximum stress in simulation of stainless steel 316L was always slightly less than experimental data, with about 2 MPa to 32 MPa. The load applied was taken from the certain percentage of ultimate strength instead of yield strength as it can used to predict the number of cycles to failure. From the results in Table 1, a stress versus number of cycle to failure was plotted between simulation and experimental results to view the significant difference of fatigue life at high stress compared to lower stress, as shown in Fig.7.

Table 1
The number of cycles to failure with load ratio (R=0.1)

Specimen	Initial load Percentage (%)	Load (KN)	Predicted Maximum stress, σ_{max} (MPa)	Predicted Number of cycle, N_f (Cycle)	Experimental Maximum stress, σ_{max} (MPa)	Experimental Number of cycle, N_f(Cycle)	Mean Stress, σ_m Experimental (MPa)	Mean Stress, σ_m predicted (MPa)
1	90%	66.87	315.50	8405	334	9256	182.00	163.5
2	80%	59.44	278.83	33542	290.93	34679	162.66	150.56
3	70%	52.01	243.45	109223	275.2	110956	142.328	110.578
4	60%	44.58	219.93	310857	234.33	329876	121.99	107.59
5	50%	37.15	218.23	885913	220.15	900893	101.66	99.74
6	40%	29.72	171.61	2066981	180.11	2067895	81.37	72.87
7	30%	22.29	168.19	9676014	160.69	9664567	61.00	68.5

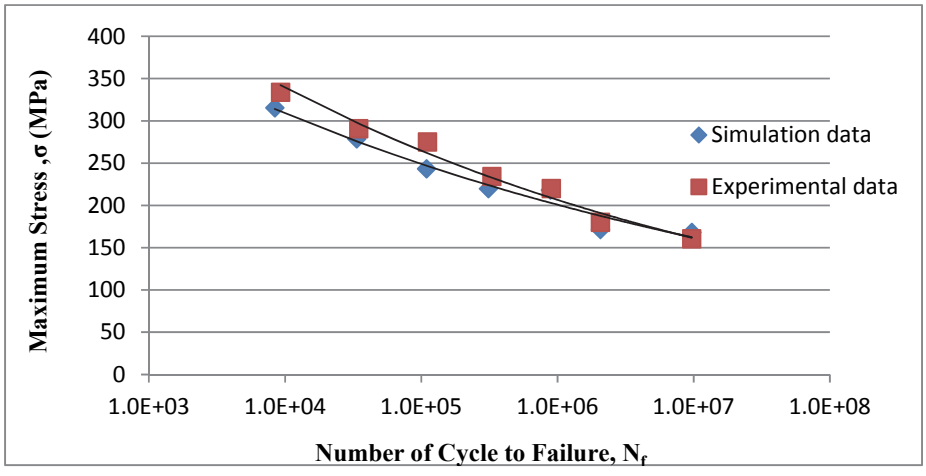

Fig. 7. S-N curve comparison of simulation data with predicted fatigue lives for Type 316L Stainless Steel

At initial condition, the specimens had subjected to loading required to achieve elongation displacement significantly with the increase in cycles. However, for another certain stage, due to the stress softening effect, the stress range might increase with increasing the number of cycles until stress softening stabilized until reaching the rupture stage. It can be seen from Fig. 7 that the maximum stress in the simulation is less than the experimental result during low cycle fatigue. However, the maximum stress value from the simulation tends to exceed the maximum stress value from the experiments in higher cycle. Overall, it has been shown that the simulation possess higher cycle of failure compare to experimental data. According to Lu et al. (2011), the number of cycles to failure that were predicted numerically were higher than the experimental data. This difference was contributed mainly by an upper stage of crack growth and more particularly, the interaction between fatigue crack growth and growth

were not counted in the numerical model. Obviously, there was a significant drop of fatigue strength in the predicted simulation analysis compared with experimental analysis. The surface irregularities of the specimen might increase the fatigue strength contrast with the predicted value, where this parameter was not taken into account for predicted simulation analysis. Generally, fatigue damage occurred and initiated at a discontinuity that acted as a stress raiser. As an indication, any parameter that would increase the local stress concentration shall also be degrading for fatigue performance. By comparing the fatigue performance of these two results under repeating cycling, it could be shown that the simulation analysis results have a longer fatigue life at lower stress ranges and shorter fatigue life at higher stress ranges than the experimental data.

6. Conclusions

This work was successfully able to design and conduct a finite element model to simulate and predict the lifespan of 316L stainless steel under ambient temperature. The fatigue lives predicted from simulations were validated and compared with experimental results, where there were slightly justified differences between the two life curves. The high stress concentration region in the simulation was indicated by high Von Mises stress at gage length of specimen and was exactly similar to the fracture surface area of specimens in the experimental validations. Simulation results showed that the maximum predicted stresses in stainless steel 316L were slightly less than those of experimental ones. Besides that, there was a drop of the predicted fatigue strength compared with experimental analysis due to materials imperfections. Overall, this model was able to predict the life span of the 316L stainless steel under cyclic loading with a great agreement with the experimental results and when the S-N curves were plotted and compared.

References

Al-Oqla, F. M., Sapuan, M. S., Ishak, M. R., & Aziz, N. A. (2014). Combined multi-criteria evaluation stage technique as an agro waste evaluation indicator for polymeric composites: date palm fibers as a case study. *BioResources*, *9*(3), 4608-4621.

Al-Oqla, F. M., Sapuan, S. M., Ishak, M. R., & Nuraini, A. A. (2015a). Predicting the potential of agro waste fibers for sustainable automotive industry using a decision making model. *Computers and Electronics in Agriculture*, *113*, 116-127.

Al-Oqla, F. M., Sapuan, S. M., Ishak, M. R., & Nuraini, A. A. (2015b). A model for evaluating and determining the most appropriate polymer matrix type for natural fiber composites. *International Journal of Polymer Analysis and Characterization*, *20*(3), 191-205.

Al-Oqla, F. M., & Sapuan, S. M. (2015). Polymer selection approach for commonly and uncommonly used natural fibers under uncertainty environments. *Jom*, *67*(10), 2450-2463.

Al-Oqla, F. M., & Omar, A. A. (2015). An expert-based model for selecting the most suitable substrate material type for antenna circuits. *International Journal of Electronics*, *102*(6), 1044-1055.

Al-Oqla, F. M., Sapuan, S. M., Anwer, T., Jawaid, M., & Hoque, M. E. (2015c). Natural fiber reinforced conductive polymer composites as functional materials: A review. *Synthetic Metals*, *206*, 42-54.

Al-Oqla, F. M., & Salit, M. S. (2017). Materials selection for natural fiber composites. *Materials Selection for Natural Fiber Composites; Elsevier: Amsterdam, The Netherlands*, 107-168.

Al-Oqla, F. M. (2017). Investigating the mechanical performance deterioration of Mediterranean cellulosic cypress and pine/polyethylene composites. *Cellulose*, *24*(6), 2523-2530.

Al-Oqla, F. M., & Sapuan, S. M. (2018). Investigating the inherent characteristic/performance deterioration interactions of natural fibers in bio-composites for better utilization of resources. *Journal of Polymers and the Environment*, *26*(3), 1290-1296.

Al-Oqla, Faris M., & El-Shekeil, Y. A. (2019). Investigating and predicting the performance deteriorations and trends of polyurethane bio-composites for more realistic sustainable design possibilities. *Journal of Cleaner Production, 222*, 865-870.

Beden, S. M., Abdullah, S., & Ariffin, A. K. (2009). Review of fatigue crack propagation models for metallic components. *European Journal of Scientific Research*, *28*(3), 364-397.

Bendersky, L., Rosen, A., & Mukherjee, A. K. (1985). Creep and dislocation substructure. *International Metals Reviews*, *30*(1), 1-16.

Hayhurst, D. R. (1972). Creep rupture under multi-axial states of stress. *Journal of the Mechanics and Physics of Solids*, *20*(6), 381-382.

Huynh, J., Molent, L., & Barter, S. (2008). Experimentally derived crack growth models for different stress concentration factors. *International Journal of Fatigue*, *30*(10-11), 1766-1786.

Finnie, I., & Heller, W. R. Creep of engineering materials 1959. *XcGraw-Hlll, London, Chapters*, 6-8.

Fan, Z. C., Chen, X. D., Chen, L., & Jiang, J. L. (2005). Fatigue-creep interaction behavior of 1.25 Cr0. 5Mo steel and condition free from creep invalidation analysis. *Multiscale Damage Related to Environment Assisted Cracking, Fracture Mechanics and Applications*, 171-176.

Fan, Z., Chen, X., Chen, L., & Jiang, J. (2006). A life prediction model of fatigue-creep interaction with stress controlled fatigue. *Journal of Pressure Equipment and Systems*, *4*, 42-47.

Fares, O., AL-Oqla, F. M., & Hayajneh, M. T. (2019). Dielectric relaxation of Mediterranean lignocellulosic fibers for sustainable functional biomaterials. *Materials Chemistry and Physics*, *229*, 174-182.

Khairul, M. A., Sapuan, S. M., AL-Oqla, F. M., Zainudin, E. S., & Rababah, M. M. (2017). Continuum damage analysis, experimental and simulation for investigating the fatigue life performance of 316L steel at high temperatures. *International Journal of Materials and Structural Integrity*, *11*(4), 175-192.

Lu, S. K., Yi, X. H., Yu, L., Jiang, Y. L., & Wei, W. R. (2011). Comparison of the simulation and experimental fatigue crack behaviors in the aluminum alloy HS6061-T6. *Procedia Engineering*, *12*, 242-247.

Maeng, W. Y., & Kang, Y. H. (1999, August). Creep-fatigue and fatigue crack growth properties of 316LN stainless steel at high temperature. In *Transactions of the 15th International Conference on Structural Mechanics in Reactor Technology (SMiRT-15)* (pp. 15-20).

Marquis, G. B., Mikkola, E., Yildirim, H. C., & Barsoum, Z. (2013). Fatigue strength improvement of steel structures by high-frequency mechanical impact: proposed fatigue assessment guidelines. *Welding in the World*, *57*(6), 803-822.

MUGHRABI, H. (2001). Assessment of fatigue damage on the basis of nonlinear compliance effects. In *Handbook of Materials Behavior Models* (pp. 622-632). Academic Press.

Niesłony, A., Kurek, A., el Dsoki, C., & Kaufmann, H. (2012). A study of compatibility between two classical fatigue curve models based on some selected structural materials. *International Journal of Fatigue*, *39*, 88-94.

Raman, S. G. S., & Radhakrishnan, V. M. (2002). On cyclic stress–strain behaviour and low cycle fatigue life. *Materials & design*, *23*(3), 249-254.

Stephens, R. I., Fatemi, A., Stephens, R. R., & Fuchs, H. O. (2000). *Metal fatigue in engineering*. John Wiley & Sons.

Tabuchi, M., Adachi, T., Yokobori Jr, A. T., Fuji, A., Ha, J., & Yokobori, T. (2003). Evaluation of creep crack growth properties using circular notched specimens. *International Journal of Pressure Vessels and Piping*, *80*(7-8), 417-425.

Velay, V., Persson, A., Bernhart, G., Bergström, J., & Penazzi, L. (2002, September). Thermal fatigue of a tool steel: experiment and numerical simulation. In *6th International Tooling Conference. Karlstad University, Sweden* (pp. 793-814).

Yıldız, F., Yetim, A. F., Alsaran, A., Celik, A., & Kaymaz, I. (2011). Fretting fatigue properties of plasma nitrided AISI 316 L stainless steel: experiments and finite element analysis. *Tribology International*, *44*(12), 1979-1986.

Zheng, M., Luo, J. H., Zhao, X. W., Bai, Z. Q., & Wang, R. (2005). Effect of pre-deformation on the fatigue crack initiation life of X60 pipeline steel. *International journal of pressure vessels and piping*, *82*(7), 546-552.